

## Historic, archived document

Do not assume content reflects current  
scientific knowledge, policies, or practices.



# MODEL STUDY OF SUPERCRITICAL FLOW CHANNEL TRANSITION FOR NICHOLS CREEK, KENEDY, TEX.

---

ARS-S-11  
July 1973



Agricultural Research Service  
UNITED STATES DEPARTMENT OF AGRICULTURE  
in cooperation with  
Oklahoma Agricultural Experiment Station  
Oklahoma State University

## CONTENTS

	Page		Page
Introduction	1	Trial I. Revised transition, warped entrance, fixed sides	12
Model study	1	Trial J. Revised transition, cylindrical entrance, fixed sides	13
Test results	4	Trial K. Revised short transition, short cylindrical entrance, fixed sides	14
Trial A. Original transition, original entrance, fixed sides	5	Trial L. Parabolic transition, parabolic entrance	16
Trial B. Original transition, original entrance, small riprap	8	Trial M. Parabolic transition, parabolic entrance, flat crest	17
Trial C. Original transition, original entrance, sunken riprap	8	Performance of original design	18
Trial D. Original transition, original entrance, large riprap	9	Effect of changing the materials on the sides of the entrance	20
Trial E. Original transition, flat crest removed from original entrance, fixed sides	9	Effect of removing flat crest from the entrance	23
Trial F. Original transition, flat crest removed from original entrance, small riprap	10	Revised single-curve transitions and effect of entrance alterations	23
Trial G. Original transition, flat crest removed from original entrance, sunken riprap	11	New parabolic transition and effect of entrance alterations	23
Trial H. Original transition, flat crest removed from original entrance, large riprap	12	Recommendations and conclusions	24
		Appendix A. The computation of Manning's $n$	25
		Appendix B. Riprap design	26

## Illustrations

Fig.	Page	Page
1. Nichols Creek transition, trials A, B, C, and D	2	8. Nichols Creek transition, trial L
2. Experimental setup for testing Nichols Creek transition model	3	9. Nichols Creek transition, trial M
3. Relative wave heights in Nichols Creek transition	6	10. Energy relationships in a reach of an open channel
4. Nichols Creek transition, trials E, F, G, and H	9	11. Average velocity against stone on channel bottom
5. Nichols Creek transition, trial I	12	12. Size of stone that will resist displacement for various velocities and side slopes
6. Nichols Creek transition, trial J	14	13. Gradation curves for dumped-stone protection
7. Nichols Creek transition, trial K	16	

## Tables

1. Dimensions of entrance and transition in trials A, B, C and D	2	12. Dimensions of entrance and transition in trial I	13
2. Velocity head coefficients at design flow of 3,950 c.f.s.	4	13. Dimensions of entrance and transition in trial J	15
3. Model Manning's $n$ for transition and exit channel	4	14. Dimensions of entrance and transition in trial K	17
4. Description of transitions and entrances in all trials	5	15. Dimensions of entrance and transition in trial L	19
5. Wave heights in trial A at design flow of 3,950 c.f.s.	6	16. Wave heights in trial L at design flow of 3,950 c.f.s.	19
6. Wave heights in the exit channel at design flow of 3,950 c.f.s.	7	17. Dimensions of entrance and transition in trial M	21
7. Water surface elevation 75 feet upstream from upstream end of the transition at design flow of 3,950 c.f.s.	8	18. Wave heights in trial M at design flow of 3,950 c.f.s.	21
8. Wave heights in trial C at design flow of 3,950 c.f.s.	8	19. Upstream water surface elevations and maximum wave heights in transition and exit channel at design flow of 3,950 c.f.s., trials A through H	22
9. Dimensions of entrance and transition in trials E, F, G and H	10	20. Upstream water surface elevations and maximum and average wave heights in transition and exit channel at design flow of 3,950 c.f.s. in trials A, E, L and M	24
10. Wave heights in trial E at design flow of 3,950 c.f.s.	11	21. Comparison of Manning's $n$ values in the transition calculated with intermediate short reaches and $n$ values calculated with a single reach	26
11. Wave heights in trial G at design flow of 3,950 c.f.s.	11	22. Riprap sizes and gradation	28

# MODEL STUDY OF SUPERCRITICAL FLOW CHANNEL TRANSITION FOR NICHOLS CREEK, KENEDY, TEX.

By D.K. McCool<sup>1</sup> and W.O. Ree<sup>2</sup>

## INTRODUCTION

The proposed canalization of Nichols Creek through Kenedy, Tex., requires a transition structure to join the existing natural earth channel with the concrete channel downstream. In making this juncture the bottom width of the structure must change from 70 feet at the upstream end to 12 feet at the downstream end, and the elevation of the invert of the structure must drop 9.37 feet. The Texas Design Office of the Soil Conservation Service, U.S. Department of Agriculture, at Fort Worth, Tex., designed a structure to provide this transition. The SCS design was a concrete chute with contracting sidewalls S-shaped in plan and with a trapezoidal cross section (fig. 1). The dimensions are given in table 1. Critical depth occurs near the upstream end of the flat crest of the entrance, and the flow is supercritical throughout the length of the transition and the exit channel.

The Soil Conservation Service requested engineers of the Water Conservation Structures Laboratory of the Agricultural Research Service in Stillwater, Okla., to review the design. The concerns of the designers were the possibilities that the structure would create undesirable back-

water upstream or that excessive wave heights would occur in the structure and in the channel downstream. Agricultural Research Service engineers undertook a model study because analytically based methods for the prediction of flow disturbances generated in transition structures were not applicable in this instance. Although Ippen and Dawson<sup>3</sup> investigated supercritical flow in channel contractions for a condition of constant specific energy and for a rectangular cross section, this transition has a gain of nearly 9 feet in specific energy in its length and is trapezoidal in cross section. Later work by Bagge and Herbich<sup>4</sup> treated transitions having changing specific energy along the flow length, as does the Nichols Creek transition, but the cross section investigated was rectangular. The difference in performance between the rectangular cross sections previously investigated and the trapezoidal cross section of this transition could be large.

The model study was conducted at the Water Conservation Structures Laboratory at Stillwater, Okla. The results of testing the original design and various revisions are presented in this report.

## MODEL STUDY

A geometrically undistorted model one twenty-fifth of the prototype was used to study the transition and its entrance. As shown in figure 2, the model was installed in a facility that included portions of the approach and exit channels.

The design discharge rate of 3,950 c.f.s. was intensively investigated, but discharge rates of 1,500 and 2,750 c.f.s. were also studied for their potential for creating excessive wave heights. In addition, one discharge rate greater than the design rate, 4,600 c.f.s., was investigated at the suggestion of the designers.

---

1. Research agricultural engineer, Palouse Conservation Field Station, Western Region, Agricultural Research Service, U.S. Department of Agriculture, Pullman, Wash. Dr. McCool was on the staff of the Stillwater laboratory when this research was done.

2. Research leader, Water Conservation Structures Laboratory, Southern Region, Agricultural Research Service, U.S. Department of Agriculture, Stillwater, Okla.

---

3. Ippen, Arthur T., Knapp, Robert T., Dawson, John H., and others. High-velocity flow in open channels. Amer. Soc. Civ. Engin. Trans. 116: 265-400, illus. 1951.

4. Bagge, Gunnar, and Herbich, John B. Transitions in supercritical open-channel flow. Amer. Soc. Civ. Engin. Hydraul. Div. Jour. 93 (HY 5):23-41, illus. 1967.



# TREATMENT OF WARPED ENTRANCE SIDES

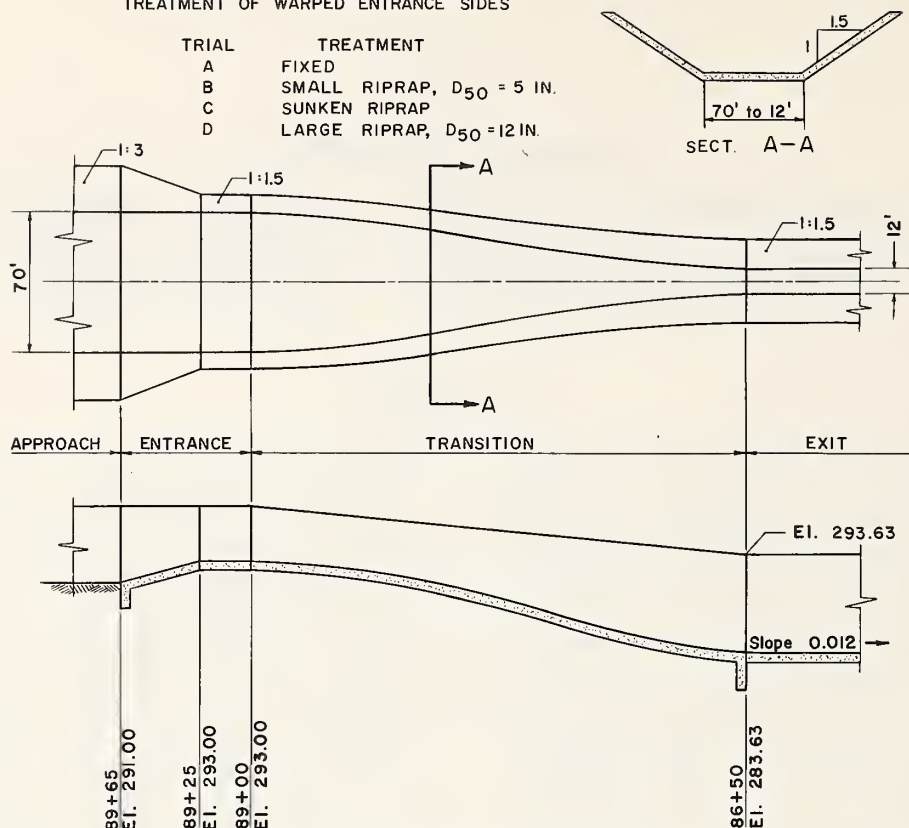


Figure 1. — Nichols Creek transition, trials A, B, C, and D. The bottom width of the 250-foot-long-transition is 70 feet at the upstream end and 12 feet at the downstream end. The 65-foot-long entrance has riprap and concrete sides and a concrete bottom. The entrance side slopes change gradually from 1 on 3 at the junction with the earth channel to 1 on 1.5 at the upstream end of the flat crest and then remain at 1 on 1.5 to the downstream end of the entrance. The concrete-lined exit channel is 12 feet wide and has 1 on 1.5 side slopes and a 0.012 bottom slope.

TABLE 1. — Dimensions of entrance and transition in trials A, B, C and D

Station	Bottom elevation	Bottom width	Side slope	Station	Bottom elevation	Bottom width	Side slope
<i>Feet</i>	<i>Feet</i>	<i>Feet</i>		<i>Feet</i>	<i>Feet</i>	<i>Feet</i>	
89+65	291.00	70.0	1 on 3	87+70	288.92	39.4	1 on 1.5
89+45	292.00	70.0	1 on 2.25	87+60	288.39	36.2	1 on 1.5
89+25	293.00	70.0	1 on 1.5	87+50	287.86	33.0	1 on 1.5
89+00	293.00	70.0	1 on 1.5	87+40	287.34	29.9	1 on 1.5
88+90	292.95	69.5	1 on 1.5	87+30	286.82	26.9	1 on 1.5
88+80	292.86	68.6	1 on 1.5	87+20	286.30	24.0	1 on 1.5
88+70	292.75	67.4	1 on 1.5	87+10	285.78	21.2	1 on 1.5
88+60	292.58	65.5	1 on 1.5	87+00	285.27	18.7	1 on 1.5
88+50	292.37	63.3	1 on 1.5	86+90	284.80	16.5	1 on 1.5
88+40	292.10	60.8	1 on 1.5	86+80	284.36	14.6	1 on 1.5
88+30	291.78	58.0	1 on 1.5	86+70	284.05	13.4	1 on 1.5
88+20	291.41	55.1	1 on 1.5	86+60	283.80	12.5	1 on 1.5
88+10	290.99	52.1	1 on 1.5	86+50	283.63	12.0	1 on 1.5
88+00	290.52	49.0	1 on 1.5	↓	↓	↓	↓
87+90	290.00	45.8	1 on 1.5	84+50	281.23	12.0	1 on 1.5
87+80	289.45	42.6	1 on 1.5				

↓ indicates linear rate of change in bottom elevation and no change in bottom width and side slope between stations.



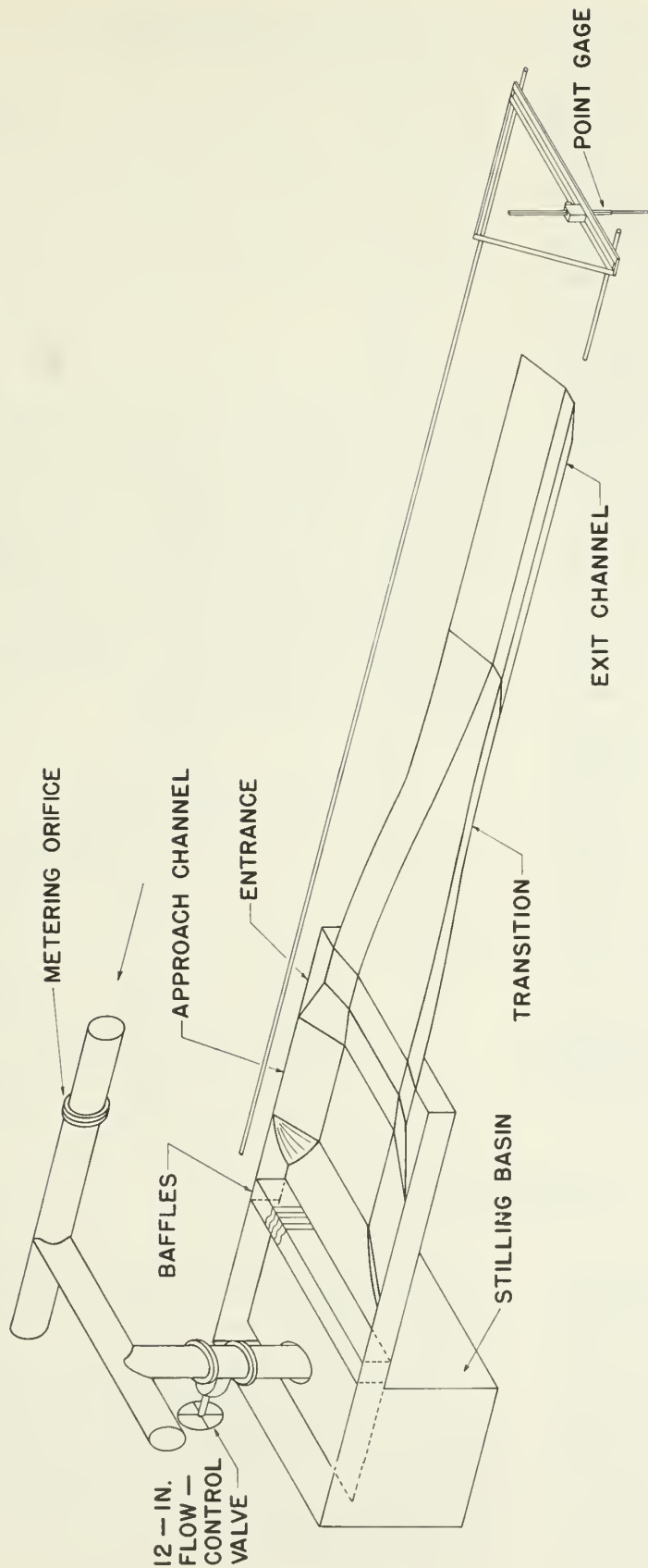


Figure 2. — Experimental setup for testing Nichols Creek transition model. The stilling basin and baffling produced nearly uniform velocity distribution in the approach channel. It was possible to install entrance sections of different lengths, shapes, and materials, including different sizes or riprap on the sides of the entrance. The transition was removable so that different lengths and shapes could be installed and tested. The flow was measured with a set of precalibrated orifice plates in the supply line. The water surface profile and wave pattern were measured with the point gage mounted on a carriage that could be moved on steel rails along the length of the model. The velocity distributions in the transition and channel were determined with a pitot tube. The transition and exit channel were constructed of plywood, which was varnished several times and waxed. The approach channel and entrance were molded of sand-cement mortar.

The first test showed an asymmetry of wave pattern. Improving the baffling did not entirely correct the flow asymmetry, so the original mortar entrance was removed and replaced with carefully constructed, laminated-redwood side pieces and a plywood bottom. This new entrance greatly reduced the asymmetry of the wave pattern.

The hydraulic roughness of the model was evaluated to insure that it was correctly scaled. Since there was a large increase in velocity from the upper to the lower end of the transition, the coefficient for the velocity head could not be assumed to be equal to unity without introducing a large error in the calculation of the energy loss. An estimate showed that the loss in energy in the transition due to friction would be of the same order of magnitude as the error in estimate of the difference in velocity heads at the two ends of the transition if an assumed velocity head coefficient was in error by as little as 0.1. An accurate determination of the hydraulic roughness of the model required measurement of velocity distribution in the flow cross section. Therefore, the velocity distribution for the design flow of 3,950 c.f.s. was measured both in the transition and in the exit channel, and velocity head coefficients were computed. The values, presented in table 2, varied from 1.08 at the upper end of the transition to 1.15 at a point in the exit channel 121 prototype feet from the downstream end of the transition. The average value of 1.11 for the velocity head coefficient,  $\alpha$ , was used in computing the total energy at the selected flow cross sections.

Manning's  $n$  was computed separately for the transition and the exit channel. The computation method is explained in appendix A. Since the roughness ratio of model  $n$  to prototype  $n$  is equal

TABLE 2. — Velocity head coefficients at design flow of 3,950 c.f.s.

Location	Velocity head coefficient, $\alpha$
Upstream end of transition	1.08
Downstream end of transition	1.10
Exit channel, 121 feet from end of transition.	1.15
Average	1.11

to the one-sixth power of the linear scale ratio, a model  $n$  of 0.0088 was required to simulate an expected  $n$  of 0.015 in the prototype. Since the  $n$  values for the model presented in table 3 were so close to the desired value, no roughening or smoothing of the model surface was required.

After the entrance baffling was adjusted and model roughness investigated, the performance of the transition and entrance was tested, and the possibility of improving the transition or decreasing its cost was studied.

TABLE 3. — Model Manning's  $n$  for transition and exit channel

Trial	Discharge	Manning's $n$	
		Transition	Exit channel
	<i>C.f.s.</i>		
B	3 975	0.0088	0.0065
	4,628	.0084	.0075
C	3,984	.0082	.0081
	4,644	.0081	.0079

## TEST RESULTS

Each modification of transition and entrance is referred to as a trial, and designated by a letter, to aid in identification and presentation of the test results. The trials are described in table 4. The results presented, except for the riprap tests, are those obtained with the design discharge, 3,950 c.f.s. Three criteria were considered in evaluating the hydraulic performance of the transitions: (1) the water surface elevation upstream from the transition, (2) the ratio of maximum depth to average depth at the measuring stations along the

channel, and (3) the ratio of maximum depth to average depth in the exit channel. The ratio of maximum depth to average depth will hereinafter be referred to as  $D_{\text{Max.}}/D_{\text{Av.}}$ .

The water surface elevations and depths of flow are given to the nearest 0.01 foot, although the values are probably accurate to only  $\pm 0.035$  foot, based on an assumed measuring accuracy of  $\pm 0.001$  foot and a rail-leveling accuracy of  $\pm 0.001$  foot, model dimensions.

TABLE 4. — Description of transitions and entrances in all trials.

Trial	Transition			Entrance
	Kind	Shape	Length <i>Feet</i>	
A	Original . . . . .	S-shaped . . . . .	250	Original, fixed sides.
B	do . . . . .	do . . . . .	250	Original, small riprap ( $D_{50}=5$ in.) on sides.
C	do . . . . .	do . . . . .	250	Original, sunken riprap.
D	do . . . . .	do . . . . .	250	Original, large riprap ( $D_{50}=12$ in.) on sides.
E	do . . . . .	do . . . . .	250	Flat crest removed from original, fixed sides.
F	do . . . . .	do . . . . .	250	Flat crest removed from original, small riprap ( $D_{50}=5$ in.) on sides.
G	do . . . . .	do . . . . .	250	Flat crest removed from original, sunken riprap.
H	do . . . . .	do . . . . .	250	Flat crest removed from original, large riprap ( $D_{50}=12$ in.) on sides.
I	Revised . . . . .	Single curve . . . . .	250	Warped, fixed sides.
J	do . . . . .	do . . . . .	250	Cylindrical, fixed sides.
K	Revised, shortened . . . . .	do . . . . .	125	Cylindrical, shortened, fixed sides.
L	New . . . . .	Parabolic . . . . .	160	Parabolic, fixed sides.
M	New . . . . .	do . . . . .	160	Parabolic, flat crest, fixed sides.

### Trial A. Original Transition, Original Entrance, Fixed Sides

The first model (fig. 1, table 1) of the original design was constructed with a smooth, fixed entrance so that any wave patterns that developed could be attributed to the geometry of the structure. This model of the original design conveyed the water satisfactorily, although the wave action was pronounced. There was some asymmetry in the wave pattern. Values of maximum, average, and dimensionless maximum flow depths for the design flow of 3,950 c.f.s. are presented in table 5. Figure 3 shows a plot of the dimensionless maximum flow depth,  $D_{Max}/D_{Av.}$ , against the dimensionless transition station,  $L/L_T$ .

Standing waves started at the beginning of the flat crest portion of the entrance (station 89+25). At this point there is a definite break in

the sidewall and in flow direction. Also, critical depth occurs quite near this station. Thus, the disturbance generated by flow separation at station 89+25 persisted as a standing wave, which crossed the chute at a pronounced angle to strike the opposite side of the transition farther downstream. The standing wave from the right side appeared to be higher than the wave from the left side. Consequently, there was asymmetry in the diamond flow pattern in the transition. The diamond wave pattern continued into the exit channel.

The maximum value of  $D_{Max}/D_{Av.}$  in the transition was 1.11. This wave height would not have exceeded the freeboard provided. In this respect the original design was deemed satisfactory.

One of the considerations in judging the performance of the transition was the extension of wave patterns into the exit channel. Normal flow

TABLE 5. — Wave heights in trial A at design flow of 3,950 c.f.s.

Station	$L/L_T$	Bottom elevation	Maximum depth	Average depth	$\frac{D_{Max.}}{D_{Av.}}$
Feet		Feet, m.s.l.	Feet	Feet	
89+00	0.00	293.00	4.20	4.10	1.024
88+80	.08	292.86	4.24	3.90	1.087
88+60	.16	292.58	4.13	3.96	1.043
88+40	.24	292.10	4.07	3.92	1.038
88+20	.32	291.41	4.49	4.03	1.114
88+00	.40	290.52	4.31	4.19	1.029
87+80	.48	289.45	4.41	4.31	1.023
87+60	.56	288.39	5.00	4.79	1.044
87+40	.64	287.34	5.45	5.28	1.032
87+20	.72	286.30	6.33	5.94	1.066
87+00	.80	285.27	7.04	6.78	1.038
86+80	.88	284.36	7.79	7.56	1.030
86+60	.96	283.80	8.28	8.00	1.035
86+50	1.00	283.63	8.32	8.12	1.025

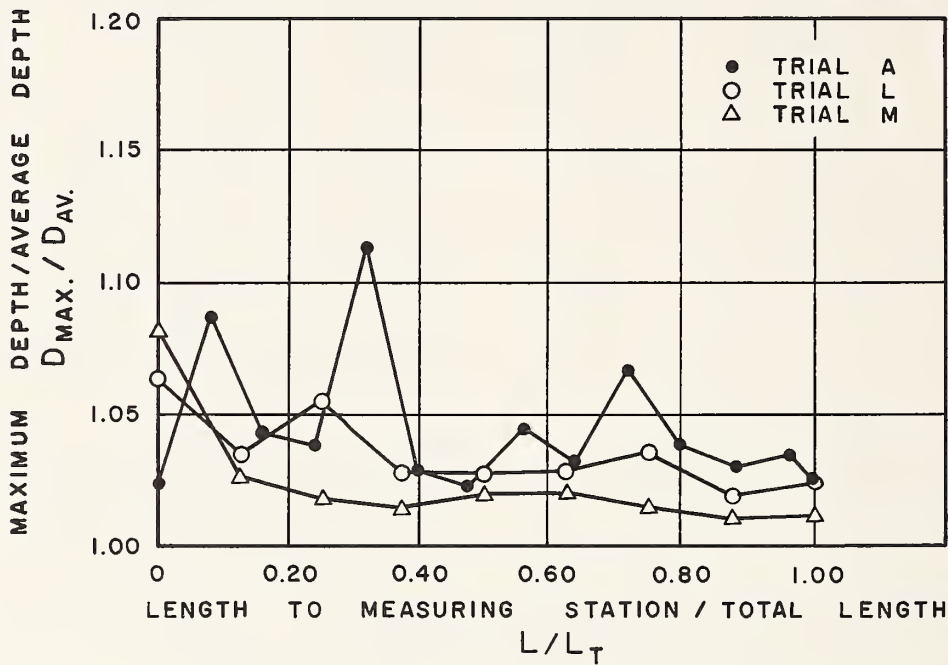


Figure 3. — Relative wave heights in Nichols Creek transition.  $L$  is the distance from the upper end of the transition to the station under consideration, and  $L-T$  is the total length of the transition.

in the exit channel is supercritical. Therefore, it is desirable to keep any disturbances in the flow entering this channel as small as possible for fear of their amplification to excessive heights by flow conditions downstream. Observed values of  $D_{Max.}/D_{Av.}$  in the exit channel are reported in table 6 for various distances downstream from the beginning of the exit channel. For trial A these distances are 25, 50, and 75 feet. For subsequent

trials these observation points were moved 100 feet downstream.

Another consideration in evaluating the performance of the transition was the upstream water surface elevation. A flax-processing mill was located approximately 400 feet upstream from the upper end of the transition, and it was necessary to keep the backwater low enough to prevent flooding. The water surface elevation 75



TABLE 6. — *Wave heights in the exit channel at design flow of 3,950 c.f.s.*

Trial	Station	Distance from downstream end of transition	Bottom elevation	Maximum depth	Average depth	$\frac{D_{\text{Max.}}}{D_{\text{Av.}}}$
	<i>Feet</i>	<i>Feet</i>	<i>Feet, m.s.l.</i>	<i>Feet</i>	<i>Feet</i>	
A	86+25	25	283.33	8.41	8.02	1.048
	86+00	50	283.03	8.14	7.91	1.028
	85+75	75	282.73	7.96	7.75	1.027
B	85+25	125	282.13	7.66	7.51	1.019
	85+00	150	281.83	7.61	7.40	1.029
	84+75	175	281.53	7.56	7.31	1.034
C	85+25	125	282.13	7.88	7.55	1.043
	85+00	150	281.83	7.81	7.36	1.061
	84+75	175	281.53	7.72	7.42	1.041
D	85+25	125	282.13	7.78	7.58	1.026
	85+00	150	281.83	7.69	7.46	1.031
	84+75	175	281.53	7.57	7.40	1.023
E	85+25	125	282.13	7.97	7.56	1.054
	85+00	150	281.83	7.65	7.47	1.024
	84+75	175	281.53	7.76	7.40	1.049
F	85+25	125	282.13	8.10	7.59	1.067
	85+00	150	281.83	7.68	7.50	1.024
	84+75	175	281.53	7.79	7.44	1.048
G	85+25	125	282.13	8.15	7.63	1.068
	85+00	150	281.83	7.80	7.55	1.033
	84+75	175	281.53	7.96	7.48	1.064
H	85+25	125	282.13	8.00	7.55	1.059
	85+00	150	281.83	7.64	7.47	1.019
	84+75	175	281.53	7.72	7.42	1.040
<sup>1</sup> I	85+25	125	282.13	8.18	8.08	1.012
	85+00	150	281.83	8.03	8.00	1.004
	84+75	175	281.53	7.99	7.92	1.010
<sup>1</sup> J	85+25	125	282.13	7.51	7.40	1.016
	85+00	150	281.83	7.44	7.33	1.016
	84+75	175	281.53	7.38	7.24	1.019
<sup>1</sup> K	85+25	125	282.13	7.06	7.01	1.007
	85+00	150	281.83	7.14	6.99	1.021
	84+75	175	281.53	7.00	6.88	1.018
L	85+35	115	282.26	7.49	7.33	1.022
	85+10	140	281.96	7.35	7.26	1.012
	84+85	165	281.66	7.42	7.24	1.025
M	85+35	115	282.26	7.48	7.36	1.016
	85+10	140	281.96	7.31	7.25	1.008
	84.85	165	281.66	7.31	7.20	1.015

<sup>1</sup> Fewer water surface readings taken across channel than in other trials.

feet from the upper end of the transition for trial A was 299.31 feet above mean sea level. This elevation was deemed acceptable by the designers and set the standard by which the performance of subsequent trials was judged. Upstream water surface elevations for various trials are presented in table 7.

TABLE 7. — *Water surface elevation 75 feet upstream from upstream end of the transition at design flow of 3,950 c.f.s.*

Trial	Water surface elevation	Trial	Water surface elevation
	<i>Feet, m.s.l.</i>		<i>Feet, m.s.l.</i>
A	299.31	H	299.24
B	299.30	I	.....
C	299.44	J	.....
D	299.39	K	.....
E	299.11	L	299.17
F	299.20	M	299.16
G	299.28		

### Trial B. Original Transition, Original Entrance, Small Riprap

Trial B (fig. 1, table 1) was conducted to determine if the rough surface of a riprapped entrance would generate different flow disturbances than the smooth entrance used in trial A and to check riprap size requirements for the entrance. The transition and entrance shape were the same as those in trial A. Selection of riprap

size and gradation followed the procedure presented in appendix B. The smallest adequate size of riprap was that with  $D_{50}=5$  inches. The selected gradation was constructed of screened crushed rock and was installed at the entrance on the warped sides. The thickness of the riprap layer was only slightly greater than 12.5 inches, the largest rock size in the gradation. Canvas was placed beneath the riprap to separate it from the gravel bed below. This permitted ready removal of the riprap and preservation of the laboriously constructed gradation for later use.

Wave profiles for the design flow of 3,950 c.f.s. were quite similar to those in trial A, so only exit channel wave height data are presented (table 6). The headwater condition was nearly the same as that in trial A (table 7).

A flow of 4,600 c.f.s. was run for 19 hours and 45 minutes (prototype time) to test the stability of the riprap. Riprap movement was negligible.

### Trial C. Original Transition, Original Entrance, Sunken Riprap

Trial C (fig. 1, table 1) tested the consequences on wave heights and patterns of the sinking or removal of the riprap at the sides of the entrance. The riprap and the canvas liner were removed. This left a 12.5-inch rise at the junction of the warped sides and the straight sides of the entrance. The exposed gravel bed was stable, and its roughness was comparable to that of riprap. During the test, large standing waves appeared in the transition. The values of  $D_{Max.}/D_{Av.}$  in the transition are presented in table 8. The maximum

TABLE 8. — *Wave heights in trial C at design flow of 3,950 c.f.s.*

Station	$L/L_T$	Bottom elevation	Maximum depth	Average depth	$\frac{D_{Max.}}{D_{Av.}}$
<i>Feet</i>		<i>Feet, m.s.l.</i>	<i>Feet</i>	<i>Feet</i>	
89+00	0.00	293.00	4.13	3.82	1.081
88+80	.08	292.86	4.49	3.87	1.160
88+60	.16	292.58	3.83	3.63	1.055
88+40	.24	292.10	3.95	3.66	1.079
88+20	.32	291.41	4.22	3.75	1.125
88+00	.40	290.52	4.49	3.93	1.142
87+80	.48	289.45	4.54	3.91	1.161
87+60	.56	288.39	5.09	4.56	1.116
87+40	.64	287.34	5.66	5.03	1.126
87+20	.72	286.30	6.44	5.86	1.099
87+00	.80	285.27	6.93	6.61	1.048
86+80	.88	284.36	7.83	7.35	1.065
86+60	.96	283.80	8.28	7.80	1.062
86+50	1.00	283.63	8.45	7.89	1.071

value is 1.16. The corresponding maximum depth is 0.62 foot higher than the average depth. The values of  $D_{Max}/D_{Av}$ . 125, 150, and 175 feet downstream from the end of the transition presented in table 6 are rather high. The water surface elevation 75 feet upstream from the upper end of the transition at 299.44 feet mean sea level is 0.13 foot higher than the value obtained in trial A (table 7). Apparently this greater height is due to additional energy loss in the entrance.

### Trial D. Original Transition, Original Entrance, Large Riprap

Riprap with  $D_{50}=5$  inches proved to be stable. Any larger size would be more so, but would its use be conservative, and would larger stones cause greater disturbances in the flow? The designers suggested trying riprap with  $D_{50}=12$  inches because the smaller size might not be available. This size of riprap was used in the entrance for this trial (fig. 1, table 1). The riprap was placed on a piece of canvas on a gravel bed.

The thickness was only slightly greater than 25 inches, the largest size in the gradation. There was no riprap movement during a prolonged flow at 4,600 c.f.s. Wave profiles at the design flow of 3,950 c.f.s. were quite similar to those in trial A, and only the data for the exit channel are presented (table 6). The headwater was slightly higher than that in trial A (table 7).

### Trial E. Original Transition, Flat Crest Removed From Original Entrance, Fixed Sides

The flat crest and parallel sidewalls downstream from the point of critical depth of the original design might adversely affect the wave pattern by keeping the flow near critical depth and enhancing wave growth, so the flat crest was removed and the contracting length of the entrance was moved 25 feet downstream to the upper end of the transition (fig. 4, table 9). This change moved the point of critical depth to the upper end of the transition.

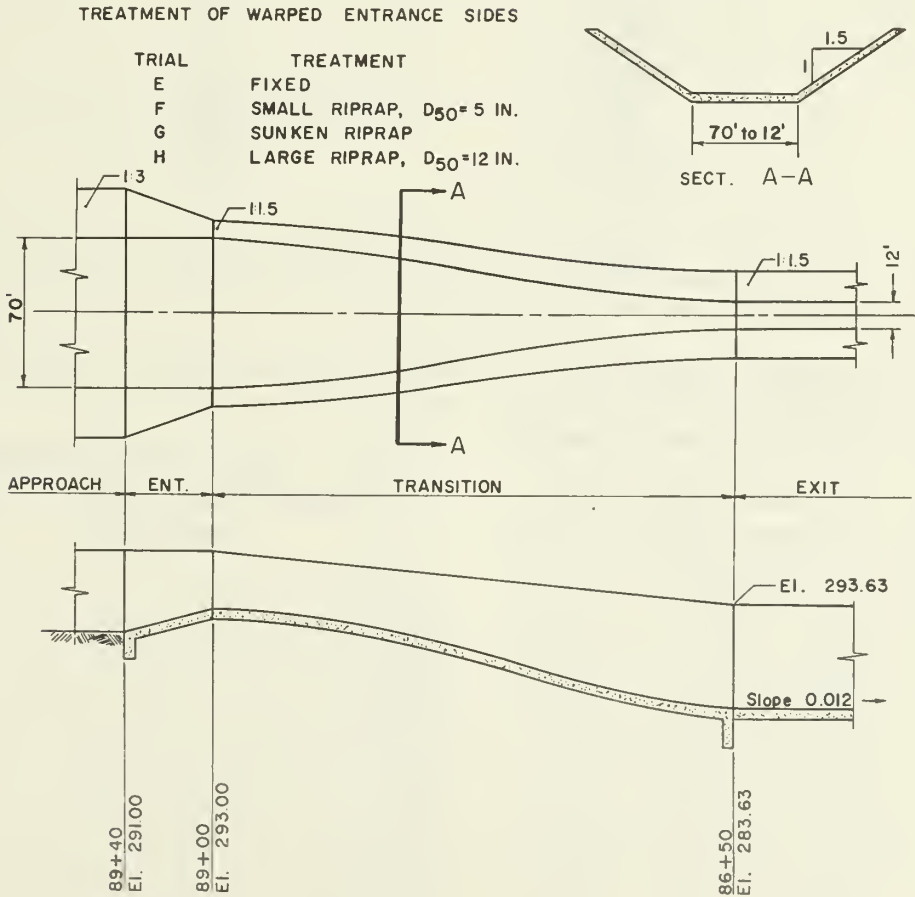


Figure 4. — Nichols Creek transition, trials E, F, G and H.



TABLE 9. — Dimensions of entrance and transition in trials E, F, G, and H

Station	Bottom elevation	Bottom width	Side slope
<i>Feet</i>	<i>Feet, m.s.l.</i>	<i>Feet</i>	
89+40	291.00	70.0	1 on 3
89+20	292.00	70.0	1 on 2.25
89+00	293.00	70.0	1 on 1.5
88+90	292.95	69.5	1 on 1.5
88+80	292.86	68.6	1 on 1.5
88+70	292.75	67.4	1 on 1.5
88+60	292.58	65.5	1 on 1.5
88+50	292.37	63.3	1 on 1.5
88+40	292.10	60.8	1 on 1.5
88+30	291.78	58.0	1 on 1.5
88+20	291.41	55.1	1 on 1.5
88+10	290.99	52.1	1 on 1.5
88+00	290.52	49.0	1 on 1.5
87+90	290.00	45.8	1 on 1.5
87+80	289.45	42.6	1 on 1.5
87+70	288.92	39.4	1 on 1.5
87+60	288.39	36.2	1 on 1.5
87+50	287.86	33.0	1 on 1.5
87+40	287.34	29.9	1 on 1.5
87+30	286.82	26.9	1 on 1.5
87+20	286.30	24.0	1 on 1.5
87+10	285.78	21.2	1 on 1.5
86+90	284.80	16.5	1 on 1.5
86+80	284.36	14.6	1 on 1.5
86+70	284.05	13.4	1 on 1.5
86+60	283.80	12.5	1 on 1.5
86+50	283.63	12.0	1 on 1.5
↓	↓	↓	↓
84+50	281.23	12.0	1 on 1.5

↓ indicates linear rate of change in bottom elevation and no change in bottom width and side slope between stations.

As in the original design, critical depth occurred quite near the location of the break in the sidewall (station 89+100 in this case). Standing waves started at this break and formed a characteristic diamond pattern down the transition. The waves were poorly defined in the upstream portion of the transition, but they intensified and became sharper as the flow entered the exit channel. Values of  $D_{Max}/D_{Av.}$  in the transition are presented in table 10. The maximum value was reduced from 1.11 in trial A to 1.08 in trial E. Corresponding values of maximum depth of flow minus average depth were reduced from 0.46 foot to 0.32 foot. In the exit channel the wave heights were greater in trial E than in trial A (table 6). Because measurements were not taken at the same station, a direct comparison cannot be made. The headwater elevation was 0.20 foot lower than that in trial A

(table 7). There was little difference in performance between trials A and E.

### Trial F. Original Transition, Flat Crest Removed From Original Entrance, Small Riprap

Since trial E had performed satisfactorily and the removal of the flat crest would reduce construction cost, it was decided to test this configuration with the riprap sides for hydraulic performance and for stability of riprap (fig. 4, table 9). The redwood side pieces for the entrance were removed and replaced with a 12.5-inch layer of the  $D_{50}=5$  inch riprap installed on canvas on a gravel base. The hydraulic performance both upstream and downstream was comparable to that in trial E (tables 6 and 7). Trial B and trial F were alike in all respects except for the flat crest.

TABLE 10. — Wave heights in trial E at design flow of 3,950 c.f.s.

Station	$L/L_T$	Bottom elevation	Maximum depth	Average depth	$\frac{D_{Max.}}{D_{Av.}}$
<i>Feet</i>		<i>Feet, m.s.l.</i>	<i>Feet</i>	<i>Feet</i>	
89+00	0.00	293.0	4.82	4.78	1.008
88+80	.08	292.86	3.88	3.73	1.042
88+60	.16	292.58	3.92	3.75	1.047
88+40	.24	292.10	4.10	3.78	1.083
88+20	.32	291.41	4.02	3.92	1.027
88+00	.40	290.52	4.22	4.04	1.045
87+80	.48	289.45	4.44	4.20	1.058
87+60	.56	288.39	4.77	4.59	1.039
87+40	.64	287.34	5.44	5.17	1.052
87+20	.72	286.30	6.02	5.85	1.028
87+00	.80	285.27	6.83	6.62	1.031
86+80	.88	284.36	7.84	7.49	1.047
86+60	.96	283.80	8.14	7.90	1.030
86+50	1.00	283.63	8.27	8.07	1.025

Removing the flat crest changed the  $D_{Max.}/D_{Av.}$  ratio from 1.03 in trial B to 1.08 in trial F. The 4,600 c.f.s.-flow was run for 17 hours and 5 minutes (prototype time). Only 60 lb. of riprap was lost.

### **Trial G. Original Transition, Flat Crest Removed From Original Entrance, Sunken Riprap**

The purpose of trial G was to determine the effect of removing the entrance riprap on the wave pattern (fig. 4, table 9). In this respect, the trial

was similar to trial C except that a flat crest was not used. The riprap and the canvas liner for the previous trial were removed, leaving a 12.5-inch rise at the junction of the entrance and the upper end of the transition. The performance was much the same as that in trial C, with the water surface being quite rough. The maximum value of  $D_{Max.}/D_{Av.}$  in the transition was 1.17 (table 11). Values of  $D_{Max.}/D_{Av.}$  in the exit channel were much the same as those in trial C (table 6). The water surface elevation 75 feet upstream from the upper end of the transition, presented in table 7, was slightly higher than that in trial E.

TABLE 11. — Wave heights in trial G at design flow of 3,950 c.f.s.

Station	$L/L_T$	Bottom elevation	Maximum depth	Average depth	$\frac{D_{Max.}}{D_{Av.}}$
<i>Feet</i>		<i>Feet, m.s.l.</i>	<i>Feet</i>	<i>Feet</i>	
89+00	0.00	293.00	5.14	5.11	1.006
88+80	.08	292.86	4.20	3.58	1.173
88+60	.16	292.58	4.26	3.83	1.112
88+40	.24	292.10	4.28	3.80	1.126
88+20	.32	291.41	4.54	3.90	1.164
88+00	.40	290.52	4.37	4.09	1.068
87+80	.48	289.45	4.65	4.20	1.107
87+60	.56	288.39	4.91	4.56	1.077
87+40	.64	287.34	5.80	5.34	1.086
87+20	.72	286.30	6.25	5.92	1.056
87+00	.80	285.27	7.14	6.77	1.055
86+80	.88	284.36	8.01	7.50	1.068
86+60	.96	283.80	8.30	7.97	1.041
86+50	1.00	283.63	8.69	8.13	1.069

## Trial H. Original Transition, Flat Crest Removed From Original Entrance, Large Riprap

The larger size riprap with  $D_{50}=12$  inches was installed at the entrance sides. Wave profiles were quite similar to those in trial E, which had the fixed entrance sides, and only the data for the exit channel are presented (table 6). The head-water condition was slightly higher than that in trial E (table 7). There was no riprap movement during a prolonged flow of 4,600 c.f.s.

## Trial I. Revised Transition, Warped Entrance, Fixed Sides

The original transition and entrance design had performed adequately. At no point had the maximum depth of flow exceeded the average depth in the cross section by as much as 20

percent. However, standing waves consistently started at the sidewall breaks in all trials. A transition with a single curve in plan and no sidewall breaks might perform better. So, temporary walls of sheet metal, curved as shown in figure 5, were placed inside the transition and were supported by spacer blocks placed on the original walls. The sheet metal was extended to the 1 on 3 side slopes of the approach channel. This resulted in a smooth, warped entrance. The dimensions of the entrance and transitions are given in table 12.

The new walls within the old narrowed the transition at its upper end. This narrowing moved the point of critical depth about 50 feet downstream into the transition. An unknown location of the critical depth complicates water surface profile computation. These consequences were not recognized at this stage in the model studies and were not taken into consideration in the next two

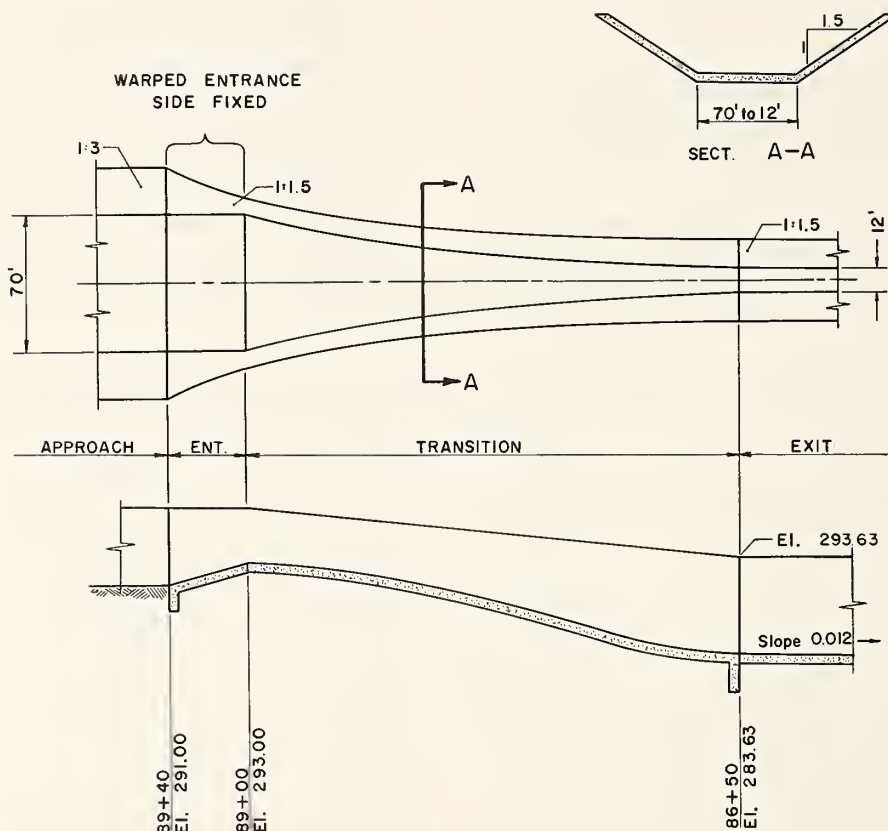


Figure 5. — Nichols Creek transition, trial I.

TABLE 12. — *Dimensions of entrance and transition in trial I*

Station	Bottom elevation	Bottom width	Side slope
<i>Feet</i>	<i>Feet, m.s.l.</i>	<i>Feet</i>	
89+40	291.00	70.0	
↓	↓	↓	1 on 3 Warped.
89+00	293.00	68.5	1 on 1.5
88+90	292.94	64.67	1 on 1.5
88+80	292.86	61.25	1 on 1.5
88+70	292.75	58.00	1 on 1.5
88+60	292.58	54.92	1 on 1.5
88+50	292.37	51.87	1 on 1.5
88+40	292.10	48.83	1 on 1.5
88+30	291.78	45.96	1 on 1.5
88+20	291.41	43.33	1 on 1.5
88+10	290.99	40.83	1 on 1.5
87+90	290.00	36.04	1 on 1.5
87+80	289.45	33.79	1 on 1.5
87+70	288.92	31.62	1 on 1.5
87+60	288.39	29.54	1 on 1.5
87+50	287.86	27.42	1 on 1.5
87+40	287.34	25.33	1 on 1.5
87+30	286.82	23.37	1 on 1.5
87+20	286.30	21.58	1 on 1.5
87+10	285.78	19.62	1 on 1.5
87+00	285.27	17.79	1 on 1.5
86+90	284.80	16.17	1 on 1.5
86+80	284.36	14.58	1 on 1.5
86+70	284.05	13.40	1 on 1.5
86+60	238.80	12.50	1 on 1.5
86+50	283.63	12.00	1 on 1.5
↓	↓	↓	↓
84+50	281.23	12.00	1 on 1.5

↓ indicates linear rate of change in bottom elevation, linear rate of change in bottom width at upstream end and constant bottom width at downstream end, and constant side slope between stations.

modifications, trials J and K. However, useful information on transition behavior was obtained during the tests, and the data are reported.

Fewer readings were taken on the water surface during the tests in this trial than in the others. Thus, values of  $D_{\text{Max.}}/D_{\text{Av.}}$  are not directly comparable to those obtained with a greater number of readings. However, the lower values obtained from this trial were confirmed by

visual evidence, which showed smaller waves than those in the original transition.

### **Trial J. Revised Transition, Cylindrical Entrance, Fixed Sides**

Trial I had performed quite satisfactorily, but the warped entrance would be difficult to describe mathematically and hence to form and construct.



Therefore, the entrance was altered slightly by bending the sheet metal so that all elements in the entrance sides had a 1 on 1.5 slope normal to the transition centerline. This cylindrical surface was continued to an intersection with the 1 on 3 sloping sidewalls of the approach channel (fig. 6, table 13).

This transition performed much the same as did the transition used in trial I. Only a minimum amount of data was collected, so values of  $D_{Max}/D_{Av.}$  are available only for the exit channel (table 6), and these are from rather limited data. These values indicate that this transition and entrance did not perform quite as well as the trial I configuration. However, the differences in performance were quite small, and trial J was adopted for further development because of its convenient construction features.

### Trial K. Revised Short Transition, Short Cylindrical Entrance, Fixed Sides

The revised transitions performed well. However, a shorter entrance and transition might perform as well and offer some construction savings. So, to investigate this possibility a shortened transition and entrance were designed by halving all the longitudinal distances of trial J. This resulted in a 125-foot transition with a 20-foot entrance (fig. 7, table 14). The visible results of testing this transition indicated that the contraction was too great. The waves in the downstream channel were rather prominent, although this is not shown by the limited data in table 6. This transition had too much contraction and insufficient drop at the upper end, as critical depth did not occur at the upstream end of the transition, but instead at a point downstream.

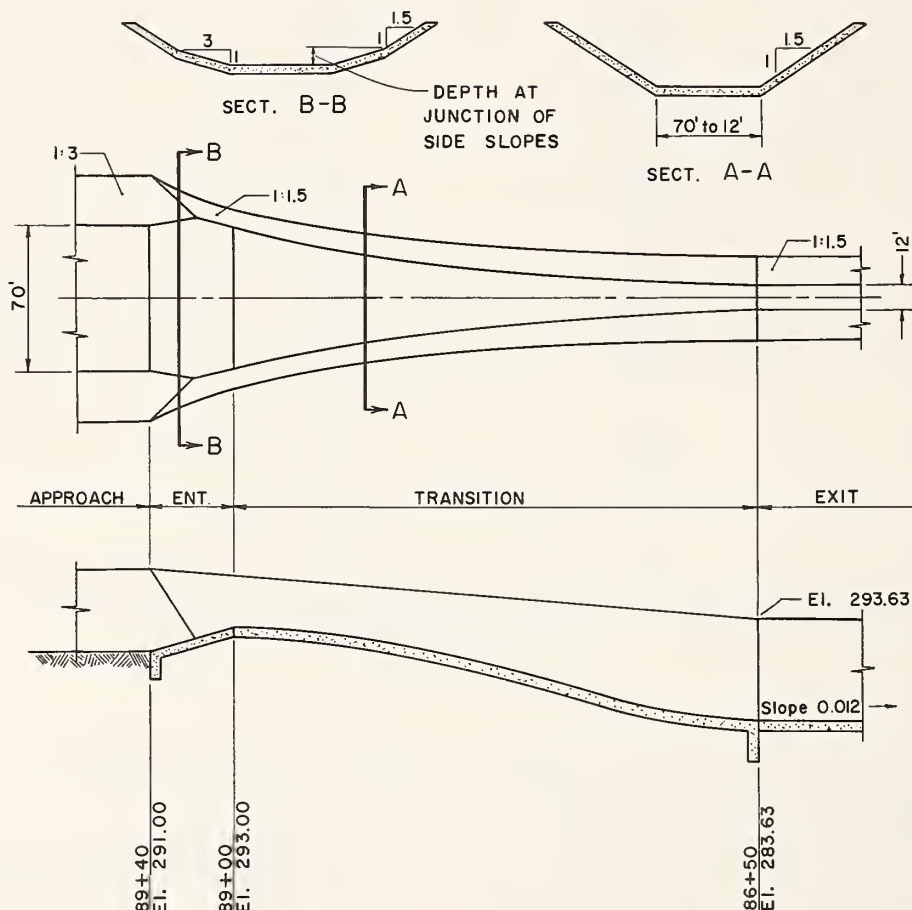


Figure 6. — Nichols Creek transition, trial J.

TABLE 13. — Dimensions of entrance and transition in trial J

Station	Bottom elevation	Bottom width	Side slope	Depth at juncture of compound side slopes
<i>Feet</i>	<i>Feet, m.s.l.</i>	<i>Feet</i>		<i>Feet</i>
89+40	291.00	70.00	Compound <sup>1</sup>	9.11
89+30	291.50	73.00	do	4.17
89+20	292.00	76.00	do	.45
89+18.5	292.08	76.50	do	.00
89+10	292.50	72.00	1 on 1.5	
89+00	293.00	68.50	1 on 1.5	
89+90	292.94	64.67	1 on 1.5	
88+80	292.86	61.25	1 on 1.5	
88+70	292.75	58.00	1 on 1.5	
88+60	292.58	54.92	1 on 1.5	
88+50	292.37	51.87	1 on 1.5	
88+40	292.10	48.83	1 on 1.5	
88+00	290.52	38.33	1 on 1.5	
88+30	291.78	45.96	1 on 1.5	
88+20	291.41	43.33	1 on 1.5	
88+10	290.99	40.83	1 on 1.5	
88+00	290.52	38.33	1 on 1.5	
87+90	290.00	36.04	1 on 1.5	
87+80	289.45	33.79	1 on 1.5	
87+70	288.92	31.62	1 on 1.5	
87+60	288.39	29.54	1 on 1.5	
87+50	287.86	27.42	1 on 1.5	
87+40	287.34	25.33	1 on 1.5	
87+30	286.82	23.37	1 on 1.5	
87+20	286.30	21.58	1 on 1.5	
87+10	285.77	19.62	1 on 1.5	
87+00	285.28	17.79	1 on 1.5	
86+90	284.80	16.17	1 on 1.5	
86+80	284.36	14.58	1 on 1.5	
86+70	284.05	13.40	1 on 1.5	
86+60	283.80	12.50	1 on 1.5	
86+50	283.63	12.00	1 on 1.5	
↓	↓	↓	↓	
84+50	281.23	12.00	1 on 1.5	

<sup>1</sup> 1 on 1.5 above; 1 on 3 below.

↓ indicates linear rate of change in bottom elevation and no change in bottom width and side slope between stations.

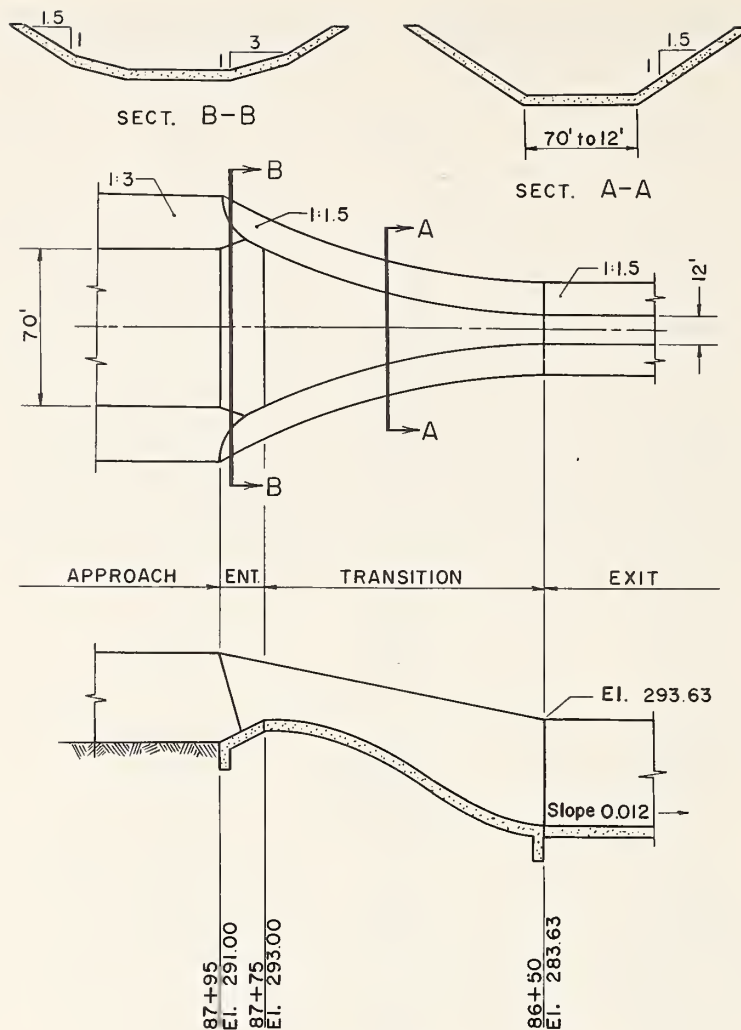


Figure 7. — Nichols Creek transition, trial K.

### Trial L. Parabolic Transition, Parabolic Entrance

The 125-foot transition length of the previous trial was too short, so the transition for trial L was made 160 feet long. At this length and at the design flow the convergence angle of the water's edge with the centerline at the start of the transition is approximately  $28^\circ$ , a maximum tolerable angle. The single wall curve that produced the smaller wave heights in trials I, J, and K was retained, but it was designed with a mathematical shape instead of being laid out by eye. The curve was a parabola with its vertex at the downstream end of the transition and 6 feet from the centerline. The parabola passed through

a point 160 feet upstream and 35 feet from the centerline. The parabolic form was carried into the entrance until it intersected the approach channel. The bottom elevations were selected by a trial-and-error design procedure, with the objectives being a smooth change of cross-sectional area and a continuously increasing Froude number in the downstream direction. Additional constraints were a bottom slope steep at the upper end and asymptotic to the exit channel bottom slope at the lower end. The adverse slope at the entrance ramp was 1 on 15.

Standing waves started at each side of the upper end of the transition. They crossed the transition diagonally, to be reflected back by the opposite side. The resulting diamond wave



TABLE 14. — Dimensions of entrance and transition in trial K

Station	Bottom elevation	Bottom width	Side slope	Depth at juncture of compound side slopes
<i>Feet</i>	<i>Feet, m.s.l.</i>	<i>Feet</i>		<i>Feet</i>
87+95	291.00	70.00	Compound <sup>1</sup>	9.11
87+90	291.50	73.00	... do ...	4.17
87+85	292.00	76.00	... do ...	.45
87+84.25	292.08	76.50	... do ...	.00
87+80	292.50	72.00	1 on 1.5	...
87+75	293.00	68.50	1 on 1.5	...
87+65	292.86	61.25	1 on 1.5	...
87+55	292.58	54.92	1 on 1.5	...
87+45	292.10	48.83	1 on 1.5	...
87+35	291.41	43.33	1 on 1.5	...
87+25	290.52	38.33	1 on 1.5	...
87+15	289.45	33.79	1 on 1.5	...
87+05	288.40	29.54	1 on 1.5	...
86+95	287.34	25.33	1 on 1.5	...
86+85	286.30	21.58	1 on 1.5	...
86+75	285.27	17.79	1 on 1.5	...
86+65	284.36	14.58	1 on 1.5	...
86+55	283.80	12.50	1 on 1.5	...
86+50	283.63	12.00	1 on 1.5	...
↓	↓	↓	↓	
84+50	281.23	12.00	1 on 1.5	...

<sup>1</sup> 1 on 1.5 above; 1 on 3 below.

↓ indicates linear rate of change in bottom elevation and no change in bottom width and side slope between stations.

pattern was well defined in the transition, but less so in the exit channel. The values of  $D_{\text{Max.}}/D_{\text{Av.}}$  in the transition are presented in table 16 and are plotted on figure 3. The maximum value was 1.06 at the upper end. The values of  $D_{\text{Max.}}/D_{\text{Av.}}$  in the exit channel were lower than those in the original design, trial A (table 6). The headwater elevation was 0.14 foot lower than that in the original design (table 7).

### Trial M. Parabolic Transition, Parabolic Entrance, Flat Crest

An attempt was made to improve the performance at the upper end of the transition by decreasing the rate of reduction of the flow cross section in the entrance. A 10-foot flat crest was

placed in the entrance just upstream from the upper end of the transition, and the 1 on 15 approach ramp was moved upstream 10 feet (fig. 9, table 17). It was thought that the critical depth would remain at the beginning of the transition because of the shortness of the flat crest and the steep slope of the transition at this point.

Values of the ratio  $D_{\text{Max.}}/D_{\text{Av.}}$  in the transition are presented in table 18 and are plotted in figure 3. The wave pattern in the transition in trial M was similar to that observed in trial L, but the wave heights were smaller. Figure 3 shows a comparison of  $D_{\text{Max.}}/D_{\text{Av.}}$  values for trials L and M and also for trial A. The smaller wave heights in the transition in trial M are evident in this plotting. Only at the upper end of the transition ( $L/L_T=0$ ), is there a higher value of the

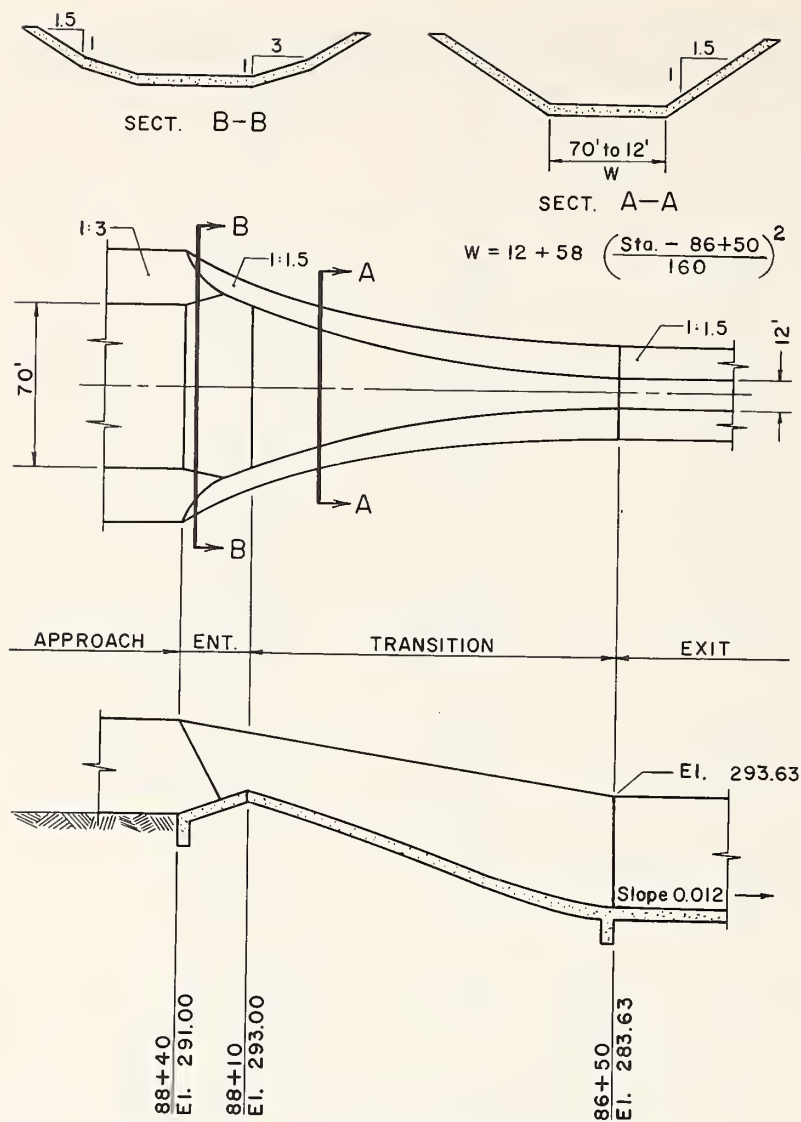


Figure 8. — Nichols Creek transition, trial L.

ratio for M than for L. However, the difference is small.

The values of  $D_{Max}/D_{Av}$  in the exit

channel were lower than in trial L (table 6). The headwater elevation was not increased by the presence of the flat crest (table 7).

## PERFORMANCE OF ORIGINAL DESIGN

Trial A, the original design, provided an adequate transition between the creek and the concrete channel downstream. In trial A waves were present in both the transition and the exit channel. However, the waves would have been contained by the normal freeboard provided in the design.

The water surface elevation 75 feet upstream from the trial A transition was 299.31 feet above mean sea level. At this elevation, the water would not flood an existing flax-processing plant upstream, and this elevation was set as the desired criterion of performance for other trials.

TABLE 15. — Dimensions of entrance and transition in trial L

Station	Bottom elevation	Bottom width	Side slope	Depth at juncture of compound side slopes
<i>Feet</i>	<i>Feet, m.s.l.</i>	<i>Feet</i>		<i>Feet</i>
88+40	291.00	70.00	Compound <sup>1</sup>	7.60
88+30	291.67	74.00	do	3.60
88+20.75	292.28	77.70	do	.00
88+20	292.33	77.20	1 on 1.5	
88+10	293.00	70.00	1 on 1.5	
88+00	292.50	63.20	1 on 1.5	
87+90	291.95	56.80	1 on 1.5	
87+80	291.35	50.80	1 on 1.5	
87+70	290.70	45.30	1 on 1.5	
87+60	290.03	40.20	1 on 1.5	
87+50	289.33	35.50	1 on 1.5	
87+40	288.61	31.20	1 on 1.5	
87+30	287.87	27.40	1 on 1.5	
87+20	287.15	24.00	1 on 1.5	
87+10	286.45	21.00	1 on 1.5	
87+00	285.75	18.40	1 on 1.5	
86+90	285.10	16.30	1 on 1.5	
86+80	284.54	14.60	1 on 1.5	
86+70	284.10	13.30	1 on 1.5	
86+60	283.79	12.40	1 on 1.5	
86+50	283.64	12.00	1 on 1.5	
↓	↓	↓	↓	
84+50	281.24	12.00	1 on 1.5	

<sup>1</sup> 1 on 1.5 above; 1 on 3 below.

↓ indicates linear rate of change in bottom elevation and no change in bottom width and side slope between stations.

TABLE 16. — Wave heights in trial L at design flow of 3,950 c.f.s.

Station	$L/L_T$	Bottom elevation	Maximum depth	Average depth	$\frac{D_{Max.}}{D_{Av.}}$
<i>Feet</i>	<i>Feet</i>	<i>Feet, m.s.l.</i>	<i>Feet</i>	<i>Feet</i>	
88+10	0.000	293.00	5.43	5.10	1.065
87+90	.125	291.95	4.69	4.53	1.035
87+70	.250	290.70	5.14	4.87	1.055
87+50	.375	289.33	5.51	5.36	1.028
87+30	.500	287.87	6.10	5.94	1.027
87+10	.625	286.45	6.71	6.53	1.028
86+90	.750	285.10	7.38	7.12	1.036
86+70	.875	284.10	7.65	7.51	1.019
86+50	1.000	283.64	7.74	7.56	1.024

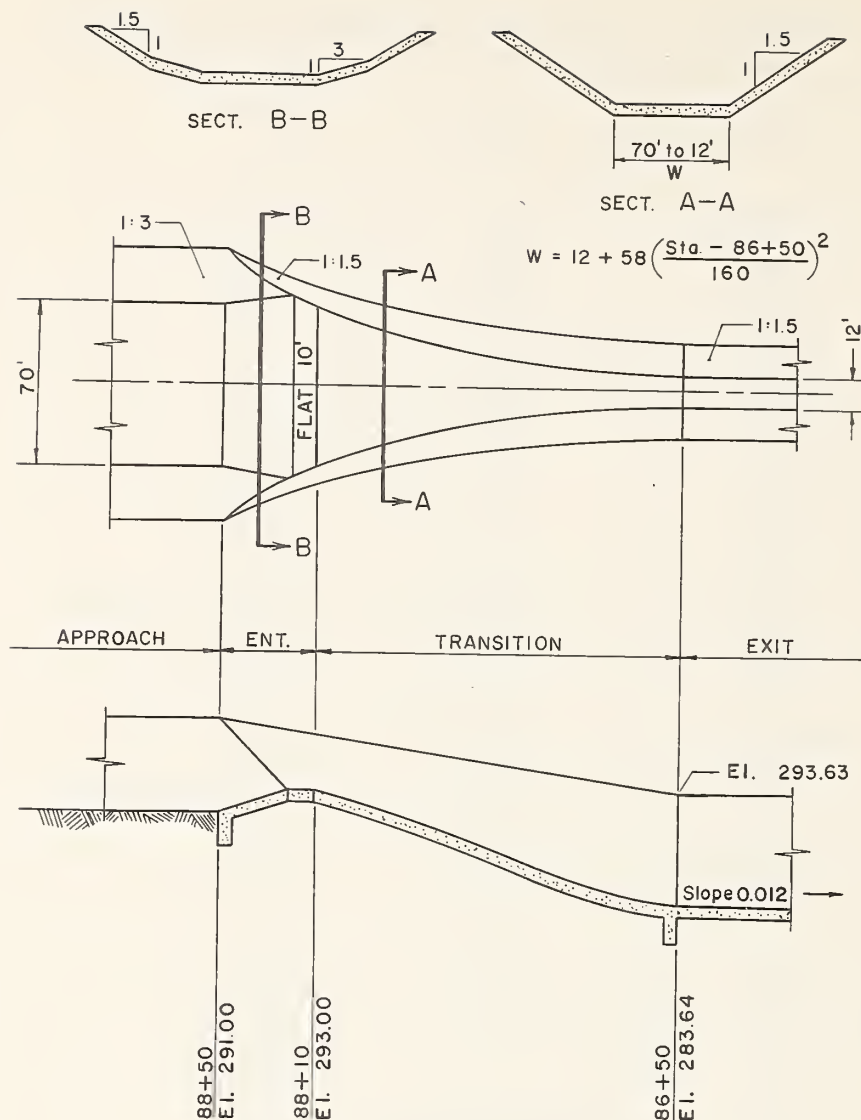


Figure 9. — Nichols Creek transition, trial M.

## EFFECT OF CHANGING THE MATERIALS ON THE SIDES OF THE ENTRANCE

Summarized values of pertinent criteria to evaluate the hydraulic performance of trials A through H are presented in table 19. When the upstream water surface elevations given in this table are compared, it should be borne in mind that a measurement accuracy of  $\pm 0.035$  foot does not permit detecting differences of less than approximately 0.07 foot.

Changing the entrance sides from smooth to small riprap,  $D_{50}=5$  inches, caused no change in upstream water surface elevation in the structure with the flat crest. Compare trial A with trial B. A slight increase was detected in the structure without a flat crest; compare trial E with trial F.

Changing the entrance sides from smooth to large riprap,  $D_{50}=12$  inches, caused a small increase in upstream water surface elevation in structures with and without the flat crest. Compare trial A with trial D and trial E with trial H.

The effect of removing the riprap to simulate a sunken condition can be seen in the difference in upstream water surface elevation between trials A and C and between trials E and G. These differences are significant and reflect the additional energy loss caused by the sharp step at the entrance.

Values of the dimensionless flow depth,

TABLE 17. — Dimensions of entrance and transition in trial M

Station	Bottom elevation	Bottom width	Side slope	Depth at juncture of compound side slopes
<i>Feet</i>	<i>Feet, m.s.l.</i>	<i>Feet</i>		<i>Feet</i>
88+50	291.00	70.00	Compound <sup>1</sup>	11.07
88+40	291.67	74.00	do.	6.93
88+30	292.33	78.00	do.	2.94
88+22.5	292.83	81.00	do.	.00
88+20	293.00	79.20	1 on 1.5	
88+10	293.00	70.00	1 on 1.5	
88+00	292.50	63.20	1 on 1.5	
87+90	291.95	56.80	1 on 1.5	
87+80	291.35	50.80	1 on 1.5	
87+70	290.70	45.30	1 on 1.5	
87+60	290.03	40.20	1 on 1.5	
87+50	289.33	35.50	1 on 1.5	
87+40	288.61	31.20	1 on 1.5	
87+30	287.87	27.40	1 on 1.5	
87+20	287.15	24.00	1 on 1.5	
87+10	286.45	21.00	1 on 1.5	
87+00	285.75	18.40	1 on 1.5	
86+90	285.10	16.30	1 on 1.5	
86+80	284.54	14.60	1 on 1.5	
86+70	284.10	13.30	1 on 1.5	
86+60	283.79	12.40	1 on 1.5	
86+50	283.64	12.00	1 on 1.5	
↓	↓	↓	↓	
84+50	281.24	12.00	1 on 1.5	

<sup>1</sup> 1 on 1.5 above; 1 on 3 below.

↓ indicates linear rate of change in bottom elevation and no change in bottom width and side slope between stations.

TABLE 18. — Wave heights in trial M at design flow of 3,950 c.f.s.

Station	$L/L_T$	Bottom elevation	Maximum depth	Average depth	$\frac{D_{Max.}}{D_{Av.}}$
<i>Feet</i>		<i>Feet, m.s.l.</i>	<i>Feet</i>	<i>Feet</i>	
88+10	0.000	293.00	5.21	4.81	1.083
87+90	.125	291.95	4.68	4.56	1.026
87+70	.250	290.70	5.01	4.92	1.018
87+50	.375	289.33	5.54	5.46	1.015
87+30	.500	287.87	6.16	6.04	1.020
87+10	.625	286.45	6.74	6.61	1.020
86+90	.750	285.10	7.30	7.19	1.015
86+70	.875	284.10	7.72	7.64	1.010
86+50	1.000	283.64	7.76	7.67	1.012

TABLE 19. -- Upstream water surface elevations and maximum wave heights in transition and exit channel at design flow of 3,950 c.f.s. trials A through H

With 25 foot flat crest, original transition, original entrance		Flat crest removed, original transition, revised entrance						
Entrance sides	Trial	Upstream water surface elevation	Maximum value, $D_{Max}/D_{Av.}$ transition	Maximum value, $D_{Max}/D_{Av.}$ exit channel	Trial	Upstream water surface elevation	Maximum value, $D_{Max}/D_{Av.}$ transition	Maximum value, $D_{Max}/D_{Av.}$ exit channel
Fixed, smooth	A	<i>Feet, m.s.l.</i> 299.31	1.114	1.048	E	<i>Feet, m.s.l.</i> 299.11	1.083	1.054
Riprap, $D_{50}=5$ in.	B	299.30	(2)	1.034	F	299.20	(2)	1.067
Sunken riprap	C	299.44	1.161	1.061	G	299.28	1.173	1.068
Riprap, $D_{50}=12$ in.	D	299.39	(2)	1.031	A	299.24	(2)	1.059

<sup>1</sup> Readings taken at different distances from beginning of exit channel than those for trials B through H.

<sup>2</sup> Data not presented.



$D_{Max.}/D_{Av.}$ , from the transition and exit channel indicate the effect of the different entrance side treatments on wave heights. A measurement accuracy of  $\pm 0.035$  foot means that, at the average depths in the exit channel, differences between  $D_{Max.}/D_{Av.}$  values of less than 0.005 are not significant. Differences among the various entrance side treatments are significant by these criteria, but are not consistent, except that the largest values occurred in trials C and G, with sunken riprap in the entrance. A reason for the inconsistency might be that water surface readings were taken at even intervals across the channel, and it would be possible to miss the point of maximum depth.

A measurement accuracy of  $\pm 0.035$  foot also means that, at the average depths near the upstream end of the transition, differences between  $D_{Max.}/D_{Av.}$  values of less than 0.011 are not significant. The values of  $D_{Max.}/D_{Av.}$  from the

transition indicate that there is a small, but significant, increase in wave heights caused by the abrupt corner at the upstream end of the transition in trials C and G with the sunken riprap. Photographs and visual observations taken at the time of testing also indicate that trials C and G had greater wave heights.

Changing the surface of the sides of the entrance from smooth to rough with small riprap resulted in no increase in water surface elevation 75 feet upstream from the upper end of the transition. However, a change to a surface of large riprap resulted in a small increase in water surface elevation. The effect of the changes on the wave heights in the exit channel was inconsistent. Sinking or removing the riprap significantly increased the upstream water surface elevation and significantly increased the wave heights in both the transition and exit channel.

## EFFECT OF REMOVING FLAT CREST FROM THE ENTRANCE

Removing the 25-foot flat crest from the entrance resulted in an average lowering of the water surface elevation by 0.15 foot 75 feet upstream from the upper end of the transition (table 19). These differences are significant and were caused by larger energy losses between the point of measurement and the upper end of the transition when the flat crest was present. The  $D_{Max.}/D_{Av.}$  data from the exit channel show a definite pattern. An averaging of the maximum  $D_{Max.}/D_{Av.}$  values for trials A through D with the flat crest gives 1.043. The average of the maximum values for trials E through H with flat

crest removed is 1.062. The difference between these values is significant, though small. For an 8-foot depth in the exit channel this difference represents an increase of 0.15 foot in the wave heights in the exit channel with the flat crest removed.

Removing the flat crest lowered the upstream water surface elevation slightly and increased the wave heights in the exit channel. Photographs and visual observations taken at the time of testing indicate that removing the flat crest slightly decreased the wave heights in the transition.

## REVISED SINGLE-CURVE TRANSITIONS AND EFFECT OF ENTRANCE ALTERATIONS

Exploratory trials I and J were run to determine if a transition with a single curve in plan would reduce the wave heights. Measurements and visual observations indicated that the water surface was smoother than it was in the original design. Therefore, a transition having a single curve in plan and half the length of the original design was tested (trial K). Testing indicated that the contraction was too great and

that the drop in bottom elevation was insufficient near the upstream end of the transition because the elevation of the energy line at the upstream end of the transition rose to 300.01 feet. In the six trials A to H, excluding C and G, the energy line elevation here was  $299.62 \pm 0.05$  feet. Visual observation also indicated that the contraction was too great, as the waves in the exit channel were rather prominent.

## NEW PARABOLIC TRANSITION AND EFFECT OF ENTRANCE ALTERATIONS

The parabolic plan for the transitions in trials L and M was derived from the dimensions of trial J. However, a length of 160 feet was chosen, and

the slope near the upper end of the transition was steepened to insure critical depth at the upper end of the transition. Summaries of pertinent criteria



to evaluate the hydraulic performance of the transition in trials L and M, as well as in trials A and E, are presented in table 20.

The data in table 20 show that trial L performed on a par with trial E with respect to upstream water surface elevation, slightly better than A or E with respect to the wave heights in the transition, and significantly better than trials A or E with respect to wave heights in the exit channel. The plot of  $D_{Max.}/D_{Av.}$  in figure 3 and the average value of  $D_{Max.}/D_{Av.}$  from the transition in table 20 indicate that trial L was consistently better than trial A, a fact that is not as evident when only the maximum values are considered. The maximum value of  $D_{Max.}/D_{Av.}$  for trial L was observed near the upper end of the transition and is the result of the curvature of flow lines rather than waves.

Further improvement in performance was sought, and a 10-foot-long flat crest was placed in the entrance. This was trial M, the last transition tested. The data in table 20 show that the addition of the 10-foot flat crest had a negligible effect on upstream water surface elevation as compared to trial L. Wave height data for the transition show improvement from the addition of the flat crest. The maximum value of  $D_{Max.}/D_{Av.}$  is only slightly larger than that for trial L, but this value is for the first station, and the values are lower further down the transition, as can be seen in figure 3 and as shown by the average value of  $D_{Max.}/D_{Av.}$ . The average value of  $D_{Max.}/D_{Av.}$  from three stations in the exit channel was also significantly better in trial M than it was in trials A, E, or L.

TABLE 20. — Upstream water surface elevations and maximum and average wave heights in transition and exit channel at design flow of 3,950 c.f.s. in trials A, E, L, and M

	Trial	Upstream water surface elevation	$D_{\text{Max.}} / D_{\text{Av.}}$			
			Max. value, transition	Av. value, all stations, transition	Max. value, exit channel	Av. value, 3 stations, exit channel
<i>Feet</i>						
Original transition:						
With 25-foot flat crest.	A	299.31	1.114	1.045	1.048	1.035
Without flat crest.	E	299.11	1.083	1.040	1.054	1.042
New parabolic transition:						
With 10-foot flat crest.	M	299.16	1.083	1.024	1.016	1.013
Without flat crest.	L	299.17	1.065	1.035	1.025	1.020

## RECOMMENDATIONS AND CONCLUSIONS

Trial M, the 160-foot-long transition with a 10-foot flat crest in the entrance, produced the smallest waves in the exit channel and is slightly favored on this account. Trial L, similar to trial M but without the flat crest, had slightly higher wave heights in the exit channel than did trial M. However, if a 1-foot slab thickness is assumed, trial L requires about 30 yards less concrete than trial M and would be first choice on that account.

The parabolic plan is very satisfactory for

this trapezoidal transition with its large increase in specific energy along its length. The parabola has its vertex at the junction of the transition and the downstream channel and passes through the desired half-width at the upstream end. The bottom slope provides a smooth variation of area with distance and an increasing Froude number in the downstream direction. The bottom slope at the lower end is asymptotic to the bottom slope of the downstream channel.

Manning's  $n$ , a resistance coefficient, is a measure of the hydraulic roughness of a surface in contact with a flow. Since the Manning flow formula is based on a condition of uniform flow, the formula is not directly applicable to the transition under study because the flow is varied. However, experience has shown that the formula can be applied to estimate friction loss in gradually varied flow if the changes in cross section in the reach over which the formula is being applied are small. For this study, this requirement meant very short reaches would need to be selected for the tests to determine  $n$ . However, for short reaches the precise and accurate determination of the slope of the energy line, an essential element in the Manning formula, is virtually impossible. A solution to this dilemma was found in the averaging method described.

The Manning formula can be written in the form

$$n = \frac{1.486}{V} R^{2/3} \left( \frac{h_f}{L} \right)^{1/2}, \quad (1)$$

where

$V$  = mean velocity, in feet per second,

$n$  = Manning's coefficient, in feet to the one-sixth power,

$R$  = hydraulic radius, in feet,

$h_f$  = energy loss, in feet,

and  $L$  = reach length, in feet.

Thus, Manning's  $n$  can be determined if the values of  $V$ ,  $R$ ,  $h_f$ , and  $L$  are known.

An expression for  $h_f$  can be developed by rearranging the Bernoulli equation, describing the energy relationships in a reach of an open channel (fig. 10), into the form

$$h_f = \alpha_1 \frac{V_1^2}{2g} + y_1 + z_1 - (\alpha_2 \frac{V_2^2}{2g} + y_2 + z_2), \quad (2)$$

where

$\alpha$  = velocity head coefficient, dimensionless,

$y$  = depth in feet,

$z$  = height above datum, in feet,

$g$  = acceleration of gravity, in feet per second per second,

and 1 and 2 = subscripts indicating sections 1 and 2, respectively.

If an average value of  $\alpha_1$  and  $\alpha_2$  is used, equation reduces to

$$h_f = \alpha \frac{V_1^2}{2g} + y_1 + z_1 - (\alpha \frac{V_2^2}{2g} + y_2 + z_2). \quad (3)$$

The value of  $h_f$  is determined from equation 3. For a short reach, the percentage error in the determination may be large because of the difficulty in determining water surface elevation with the required accuracy and precision. However, the percentage error in the  $h_f$  determination can be reduced by using a longer reach. Therefore, closely spaced transverse measurements of water surface elevations were made at each end of the transition or channel reach to obtain a good estimate of the average water surface elevations at the end sections. Velocity distribution measurements were made at these same sections to determine  $\alpha$ . The values obtained from these measurements can be used in equation 3 to give a value of  $h_f$  for the long reach.

The use in equation 1 of the average values of  $V$  and  $R$  at the ends of the long reach is generally not suitable for nonuniform flow because it implies a linear variation of  $V$  and  $R$  with distance. The solution to the problem lies in using short, intermediate reaches for determining  $V$  and  $R$ . The method is based on the reasoning that the energy loss in a long reach is made up of the energy losses for the shorter, included reaches. This summation of losses is expressed in the equation

$$h_f = \sum h_{fi} = \sum \frac{V_i^2 n_i^2 L_i}{2.21 R_i^{4/3}}, \quad (4)$$

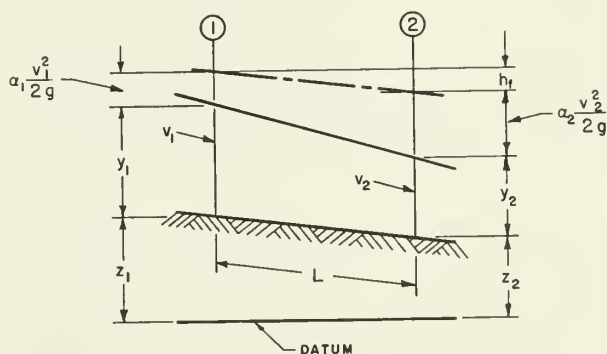


Figure 10. — Energy relationships in a Reach of an open channel.

where subscript  $i$  refers to the average values for the short lengths of channel  $L_i$  that make up a longer reach and  $h_f$  is the total energy loss for the longer reach.

If the Manning coefficient can be assumed to be constant over the long reach, then

$$h_f = n^2 \sum \frac{V_i^2 L_i}{2.21 R_i^{4/3}} \quad (5)$$

Equation 5 can be rearranged into the form

$$n = \left[ \frac{\frac{h_f}{\sum \frac{V_i^2 L_i}{2.21 R_i^{4/3}}}}{1/2} \right]^{1/2} \quad (6)$$

Equation 6 provided the basis for determining the average value of Manning's  $n$  for the transition and a reach of the downstream channel. The value of  $h_f$  is determined from the long reach by equation 3. The intermediate values of  $V$  and  $R$  are determined at the ends of short, intermediate reaches. Fewer water surface readings were needed at these intermediate cross sections than at the ends of the longer reach, because if readings are taken at several intermediate reaches, errors in the precision and accuracy of determination of  $V$  and  $R$  will tend to average out.

The Manning's  $n$  values determined by equation 6 were compared with  $n$  values calculated by simply using the average of the velocities and hydraulic radii at the two ends of the transition. The results are given in table 21.

The more elaborate computation system yielded  $n$  values with less difference between the two determinations than did the simplified computation. Without more tests the error in the determination cannot be established, so it is not known whether the differences are real. However, the smaller variation in the  $n$  values computed by the averaging method gives greater confidence in these  $n$  values.

TABLE 21. — Comparison of Manning's  $n$  values in the transition calculated with intermediate short reaches and  $n$  values calculated with a single reach

Trial	$Q$	Manning's $n$	
		From $\Sigma$ of intermediate reaches	From single reach
	<i>C.f.s.</i>		
B	3.975	0.0088	0.0090
C	3.984	.0082	.0072

## APPENDIX B. — RIPRAP DESIGN

The riprap on the sides of the entrance of the original transition was designed after a procedure suggested by Searcy<sup>5</sup> (pp. 30-33, 40-41). The procedure assumes a graded riprap and is based on the  $D_{50}$  size, that size for which 50 percent of the material is finer. The desired gradation is then based on curves published by Murphy and Grace.<sup>6</sup>

Selection of the required stone size is a trial-and-error procedure. Figure 11, derived from the so-called universal velocity distribution law, is a plot of the ratio of stone diameter to total depth of

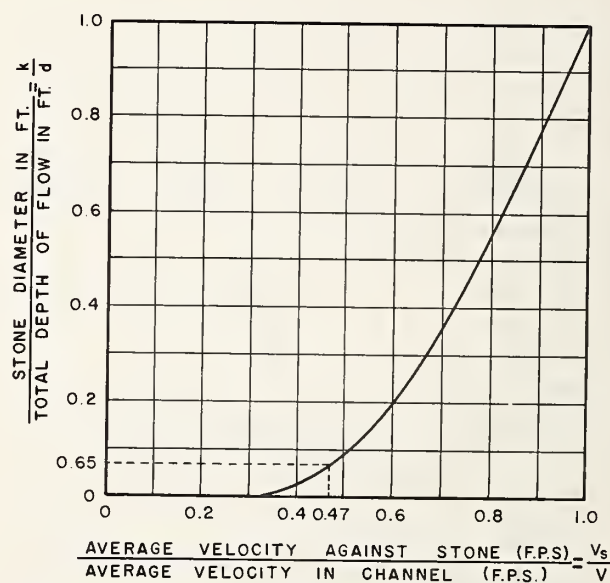


Figure 11. — Average velocity against stone on channel bottom. (From Searcy, cited in footnote 5.)

5. Searcy, James K. Design of roadside drainage channels. Hydraulic Design Series No. 4. Hydraulics Branch, Bridge Division, Bureau of Public Roads, U.S. Department of Commerce, Washington, D.C. 56 pp., illus. 1965.

6. Murphy, Thomas E., and Grace, John L., Jr. Riprap requirements for overflow embankments. Culvert and Slope Protection. Highway Res. Board Rec. No. 30: 47-55, illus. 1963.



flow versus the ratio of average velocity near the stone to average velocity in the channel. For a given depth and velocity of flow a stone size is selected for trial, and the ratio of  $V_s/V$  is determined from figure 11. Then the value of  $V_s$  is found. A second plot, figure 12, obtained empirically, is used to check if the selected stone size will resist movement. If the chosen stone size is smaller or larger than the size obtained from figure 12, a different stone size is selected for a second trial. This procedure is continued until the selected and the required sizes agree.

The desired gradation is determined by the use of figure 13. The solid lines, A and B, are "... gradation curves which were found to be very satisfactory in tests at the U.S. Army Engineer Waterways Experiment Station."<sup>7</sup> A line is laid approximately parallel to lines A and B passing through the point where a horizontal line through

7. Searcy, p. 40. Cited in footnote 5.

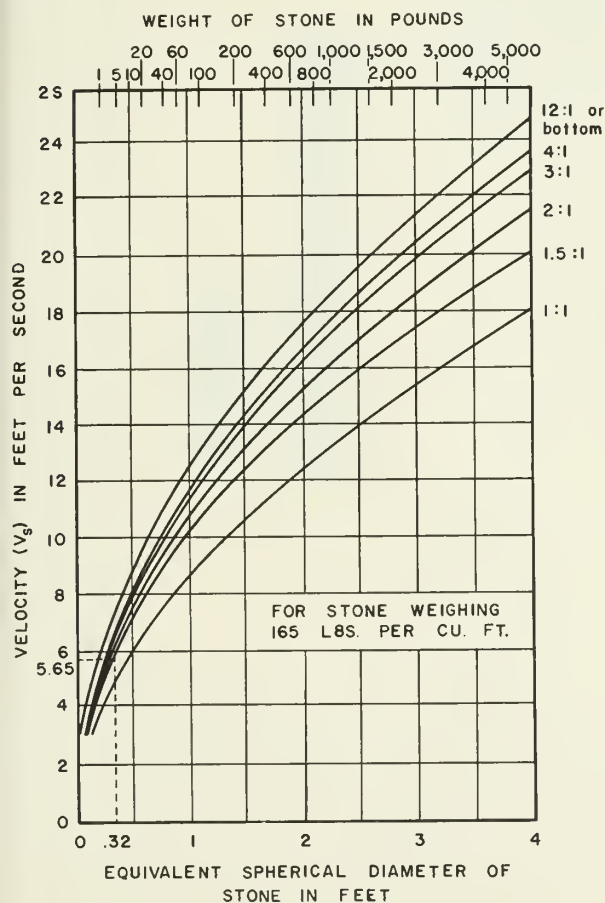


Figure 12. — Size of stone that will resist displacement for various velocities and side slopes. (From Searcy, cited in footnote 5.)

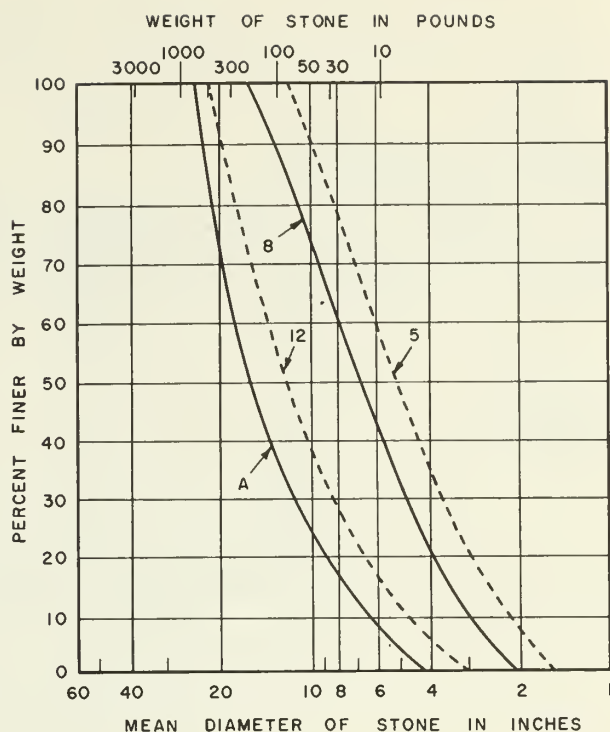


Figure 13. — Gradation curves for dumped-stone protection. (From Searcy, cited in footnote 5. Dash lines added.)

the 50 percent finer by weight mark on the ordinate would intersect a vertical line passing through the mean stone diameter (selected from figures 11 and 12) on the abscissa.

The gradation is scaled to model size by applying the length scale to the diameter. This results in a weight scale based on the cube of the length scale.

For the Nichols Creek entrance, the velocity chosen was the critical velocity at the downstream end of the riprapped reach at a flow of 4,600 c.f.s., the overload discharge chosen by the designers. The critical depth is 4.94 feet, and the mean velocity is 12 feet per second. By the trial-and-error procedure and the use of figures 11 and 12, an equivalent spherical stone diameter of 0.32 foot, or 3.84 inches, is obtained. This  $D_{50}$  size was rather arbitrarily raised to 5 inches because of the possibility of uplift due to nonhydrostatic pressure distribution in the vicinity of the control section. The required gradation is shown on figure 13. Also shown is the maximum size that would possibly be used in this installation, so it was included to test the wave-generating potential of a larger rock size. The model and prototype riprap sizes are given in table 22.

TABLE 22. — Riprap sizes and gradation

U.S. standard sieve size	Opening	Equivalent prototype size	D <sub>50</sub> =5 inches		D <sub>50</sub> =12 inches	
			Percent finer	Percent mixed	Percent finer	Percent mixed
	<i>Inches</i>	<i>Inches</i>				
1	1.00	25.0	.....		100	
3/4	.750	18.8	.....		87	13
5/8	.625	15.6	.....		72	15
1/2	.500	12.5	100		51	21
3/8	.375	9.4	88	12	37	14
5/16	.312	7.8	76	12	28	9
1/4	.250	6.2	63	13	19	9
3-1/2	.223	5.6	55	8	14	5
4	.187	4.7	45	10	9	5
5	.157	3.9	34	11	4	9
7	.111	2.8	19	15	.....	
10	.0787	2.0	7	19	.....	